1 dummy1

2 dummy2

3 dummy3

4 dummy4

4.1 dummy4.1

4.2 Radiative Transfer of the Atmosphere in the Infrared

Physical retrievals of atmospheric parameters attempt to minimize the difference between computed and observed channel radiances. The accuracy of the retrieval is therefore directly related to the accuracy of the computed radiances. AIRS measures the convolution of the up-welling monochromatic radiances with the instrument spectral response function (SRF). An exact calculation of the observed radiances therefore requires the convolution of simulated monochromatic radiances. These computed radiances are complicated functions of the atmospheric state (temperature, pressure, gas amount), the gas transmittances, and the AIRS SRFs. Since the atmospheric emission lines can have widths as small as ~ 0.001 cm^{-1}, the wavenumber grid scale for the radiance calculation must have a similar spacing. This small grid spacing, combined with the time- consuming SRF convolutions, makes a monochromatic calculation of radiances orders of magnitude too slow for practical use. Instead, we must use a fast radiative transfer model that is based on appropriately convolved atmospheric transmittances for each spectral channel. Then the radiative transfer can be performed on a per-channel basis rather than on a finely spaced monochromatic wavenumber grid.

The starting point for understanding the AIRS radiative transfer algorithm (AIRS-RTA) is the monochromatic radiative transfer equation. The monochromatic radiance leaving the top of a non-scattering atmosphere is

$$\begin{aligned} R(\nu,\theta) = \epsilon_s(\nu)B(\nu,T_s)\tau(\nu,p_s,\theta) + \int_{p_s}^{0} B(\nu,T)\frac{d\tau(\nu,p,\theta)}{dp}dp \\ +\rho_s(\nu)H_{sun}(\nu)\tau(\nu,p_s,\theta)\tau(\nu,p_s,\theta_{sun})cos(\theta_{sun}) + R_d \end{aligned} \quad (1)$$

where $B(\nu,T)$ is the Planck function emission at frequency and temperature T, $\tau(\nu,p,\theta)$ is the transmittance between pressure p and the satellite at viewing angle θ, and T_s, ϵ_s, and ρ_s refer to the Earth's surface temperature, emissivity, and reflectivity respectively. The solar radiance incident at the top of the atmosphere is represented by H_{sun}, while R_d is a relatively small radiance contribution arising from the reflection of the downwelling atmospheric thermal emission

$$R_d(\nu) \;=\; 2\pi\rho_s\tau(\nu,p_s,\theta)\int_{p=0}^{p_s} B(\nu,T)\int_{\theta_i=0}^{\pi/2} sin(\theta_i)cos(\theta_i)\frac{d\tau_d(\nu,p,\theta_i)}{dp}dpd\theta_i \tag{2}$$

where τ_d is the transmittance between pressure p and the surface. The dependence of temperature and angle on pressure (altitude) has been suppressed in the above equations, as well as the dependence of the transmittances on temperature and gas abundance.

The AIRS-RTA allows the integration of the radiative transfer equation over 100 atmospheric layers to be performed in a discrete form. For reasons of clarity and brevity we omit further discussion of the last two terms in Equation (4.2.1), except to note that they are included in the AIRS-RTA by simplified approximations. A discrete form of the radiative transfer equation can then be written conveniently as

$$R_{meas} = \int R(\nu)f(\nu-\nu_o)d\nu = \int(\epsilon_s B(T_s)\tau_N + \sum_{i=1}^{N} B(T_i)(\tau_{i-1}-\tau_i))f(\nu-\nu_o)d\nu \tag{3}$$

where the atmospheric layers are numbered from space to the surface, 1 to N respectively. $B(T_i)$ is the Planck emission for layer i at temperature T_i, τ_i is the transmittance from layer i to space, inclusive, and $f(\nu-\nu_o)$ is the AIRS SRF for the channel centered at ν_o. The emissivity and Planck function are nearly constant over the narrow width $\Delta\nu$ of the AIRS channels, so they may be moved outside the integral. After integrating the transmittances, we are left with the channel-averaged form of the radiative transfer equation,

$$R_{meas} = \epsilon_s B(T_s)\tau_N + \sum_{i=1}^{N} B(T_i)(\tau_{i-1}-\tau_i) \tag{4}$$

where all terms now represent appropriate channel-averaged quantities.

The polychromatic approximation introduced in the above relation replaces the monochromatic layer-to-space transmittances with transmittances convolved with the SRFs. This in effect convolves the outgoing radiances, allowing us to do radiative transfer at just a single frequency per channel. In most cases, the AIRS channel radiances calculated from the above equation using convolved layer-to-space transmittances differ from the convolved monochromatic AIRS channel radiances by ≤ 0.05 K, assuming one has perfect layer-to-space convolved transmittances in hand.

Figure 1 illustrates the large difference in spectral resolution between the upwelling monochromatic radiation and an AIRS brightness temperature spectrum. Because of this large difference in spectral resolution one cannot derive the layer-to-space transmittances directly from the product of the convolved layer transmittances since Beer's law is no longer valid. Overcoming this problem is one of the major issues in the development of a model for fast, parameterized, convolved layer transmittances.

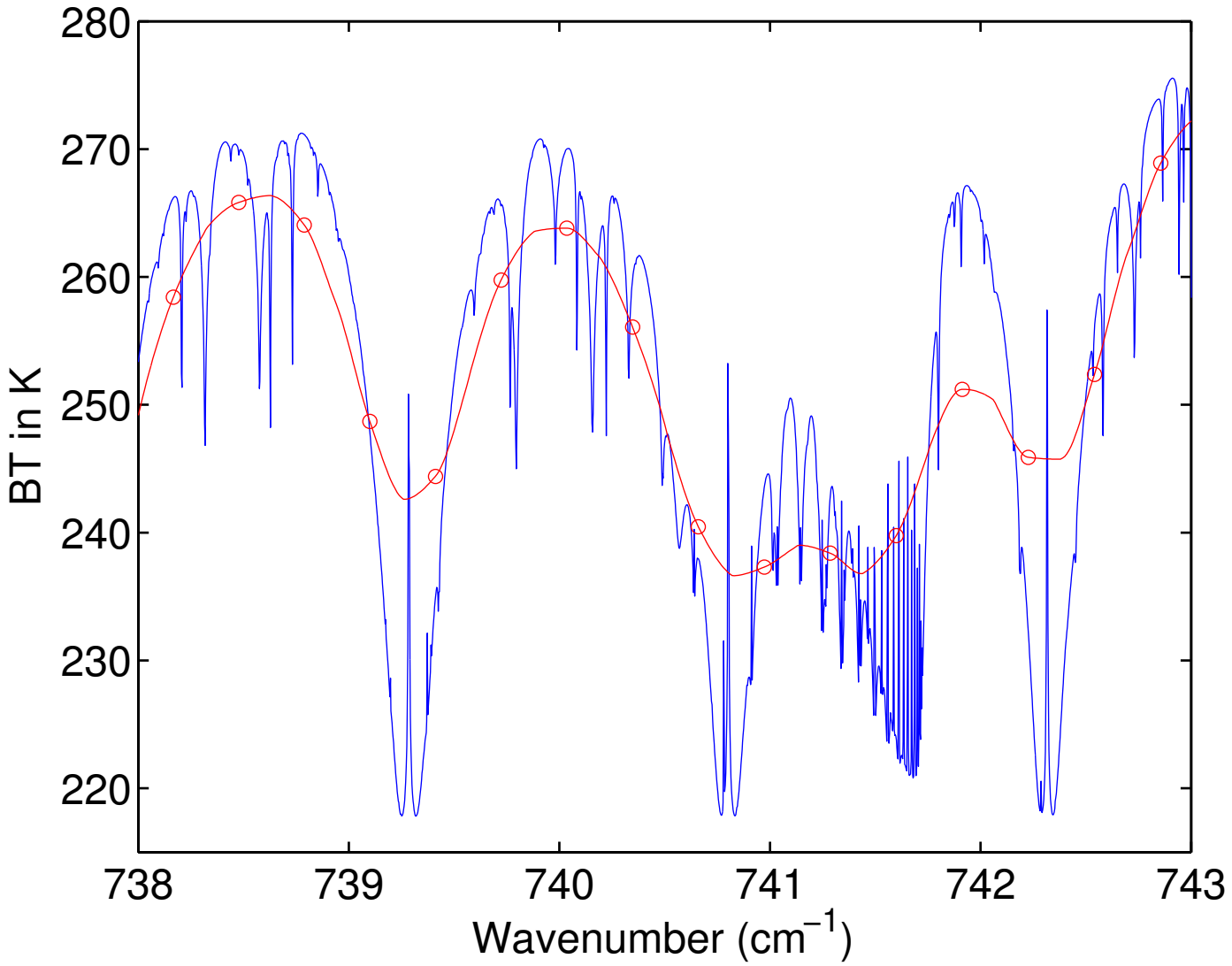

Figure 1: Simulated monochromatic (blue) and AIRS SRF convolved (red) brightness temperature spectra. The red circles indicate the actual AIRS channel centroids.

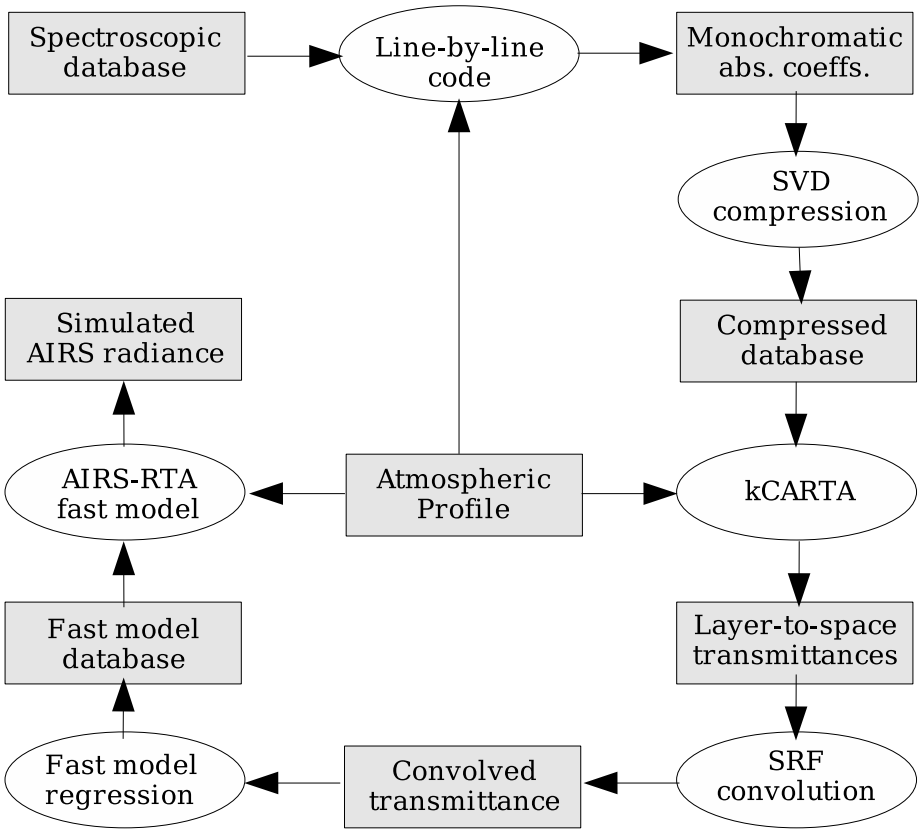

Figure 2: Flow diagram for development of the AIRS-RTA

In the following sections we discuss the major issues in developing the AIRS-RTA, which include: (1) forming a discrete grid for integrating the radiative transfer equation, (2) parameterizing the layer transmittances as a function of the atmospheric state, (3) the spectroscopy needed to compute atmospheric transmittances, (4) the line-by-line algorithm used to generate the monochromatic transmittances (5) the AIRS spectral response functions

The flowchart shown in Figure 2 outlines the flow of activities needed to develop the AIRS-RTA, which is discussed in the following text.

4.2.1 AIRS Atmospheric Layering Grid

The atmospheric pressure layering grid for the AIRS-RTA model was selected to keep radiative transfer errors below the instrument noise. Grid characteristics are a function of the spectral region(s) of

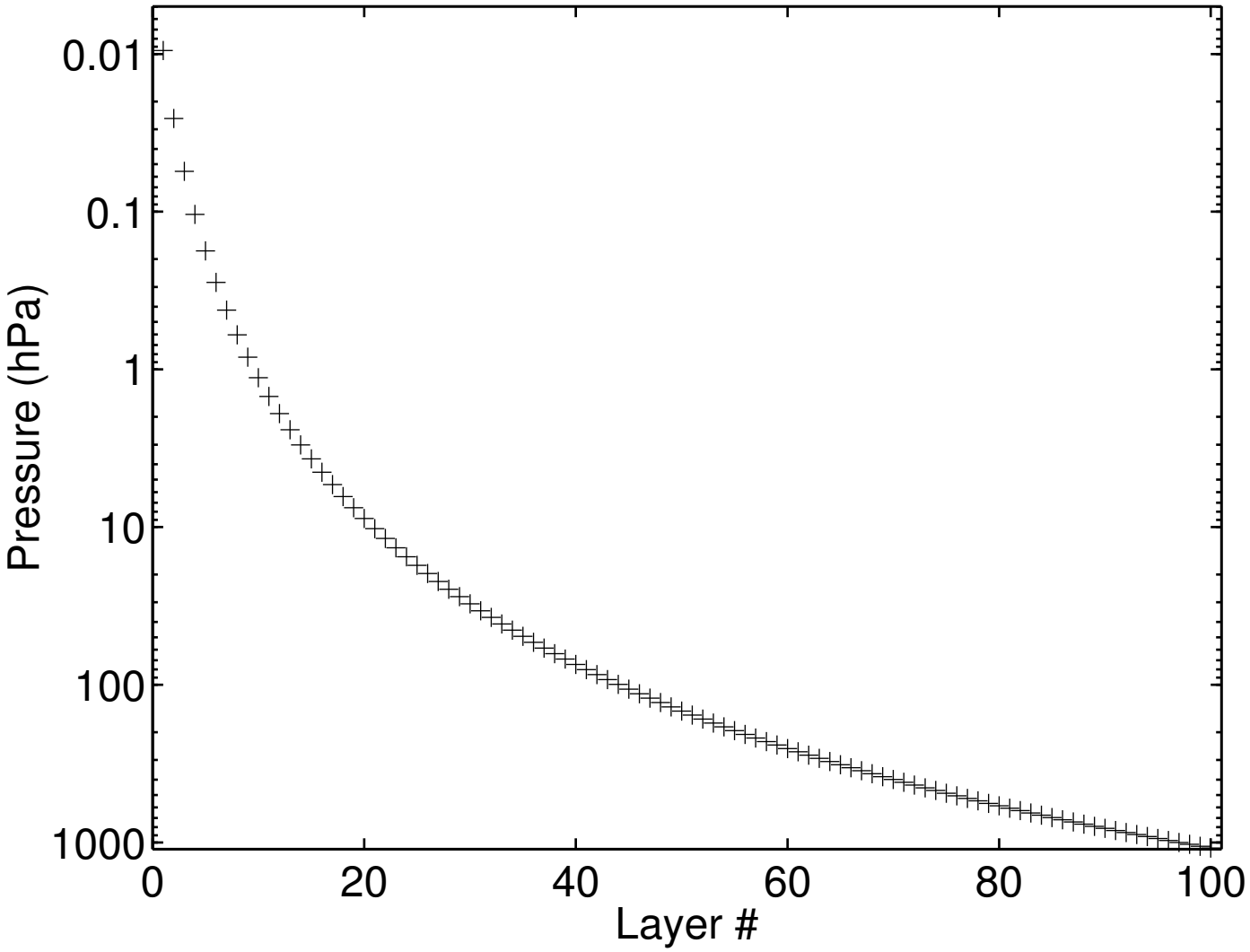

Figure 3: Mean pressure of the AIRS-RTA 100 layers

.

observation, the instrument resolution, and instrument noise. The speed of the final fast transmittance model will depend on the number of layers, so excessive layering should be avoided.

Line-by-line simulations indicate some channels need a top layer with pressures as small as 0.01 mb (an altitude of $\sim$ 80 km). The region of primary importance to AIRS is the troposphere and lower stratosphere, where layers on the order of 1/3 of the nominal 1 km vertical resolution of AIRS retrievals are desired. Smoothly varying layers facilitate interpolation and avoid large changes in layer effective transmittances. The following relation defines the pressure layer boundaries selected for AIRS:

$$P_i = (ai^2 + bi + c)^{7/2} \tag{5}$$

where P is the pressure in millibars; i is the layer boundary index and ranges from 1 to 101; and the

parameters a, b, and c were determined by solving this equation with the following fixed values: $P_1 =$ 1100 mb, $P_{38} = 300$ mb, and $P_{101} = 0.005$ mb. The 101 pressure layer boundaries in turn define the 100 AIRS layers. These layers vary smoothly in thickness from several tenths of a kilometer near the surface to several kilometers at the highest altitudes. Figure 3 is a plot of the layer mean pressure for the 100 AIRS layers.

4.2.2 Fast Transmittance Modeling

Over the years, a number of fast transmittance models have been developed for various satellite instruments [McMillin and Fleming, 1976; Fleming and McMillin, 1977; McMillin et al., 1979, 1995; Scott and Chedin, 1981; Susskind et al., 1983; Erye and Woolf, 1988; Chruy et al., 1995]. However, some of these models only have been applied to the microwave region where the measured radiances are essentially monochromatic and easier to model. AIRS required a major new effort in the development of its RTA. Some of the details of our model can be found in Strow et al. [2003].

The AIRS-RTA most closely follows Susskind et al. [1983] by parameterizing the optical depths rather than transmittances for channels where the influence of water vapor is small. Channels sensitive to water vapor are modeled using a variant of the Optical Path TRANsmittance (OPTRAN) algorithm developed by McMillin et al. [1979, 1995]. The AIRS infrared fast model is thus a hybrid of both Susskind's approach and OPTRAN.

The AIRS-RTA model actually produces equivalent channel averaged optical depths, k, which are related to the layer transmittances, τ, by $\tau = \exp(-k)$. The optical depth is the product of the absorption coefficient and the optical path. For AIRS, a fast model for k is much more accurate than a model that directly returns layer τ. k is computed for each of the 100 atmospheric layers used for AIRS radiative transfer. The current AIRS-RTA model allows water, ozone, methane, carbon monoxide, carbon dioxide, the temperature, and local scan angle to vary. All other gases are treated as "fixed" gases. These gases are "fixed" in the sense that we only need to parameterize their dependence on temperature, not amount. Although the observed radiances are primarily sensitive to temperature via the Planck function, the temperature dependence of the transmittances is also important.

The following discussion outlines the development of a parameterization of the convolved layer transmittances as a function of the atmospheric state. Most of the complications of this parameterization arise from the loss of Beer's law, which forces us to introduce terms in the transmittance parameterization for a given atmospheric layer that depend on layers above the particular layer under consideration. These parameterizations, which are functions of the atmospheric profile, are derived from least- squares fits to a statistical set of atmospheric profiles in order to ensure that we can faithfully produce the appropriate transmittances under all atmospheric conditions. We call this statistical set of profiles our "regression profiles".

Breakout of Gases Once the atmospheric layering grid and regression profiles (see later discussion) are selected, the monochromatic layer-to-space transmittance can be calculated. The gases are distributed into sub-groups that are either fixed or variable. The details of how the transmittance model simultaneously handles several variable gases is somewhat complicated and beyond the scope

of this document. For simplicity, this discussion is restricted to fixed gases (F), water vapor (W), and ozone (O). The breakout of the other variable gases is similar. The monochromatic layer-to-space transmittances for the 48 regression profiles are calculated for each pressure layer, grouped into the following three sets, and convolved with the AIRS SRF,

$$\begin{aligned} F_l &= \tau_l(fixed) \\ FO_l &= \tau_l(fixed + ozone) \\ FOW_l &= \tau_l(fixed + ozone + water) \end{aligned} \tag{6}$$

Water continuum absorption is excluded since it varies slowly with wavenumber and does not need to be convolved with the AIRS SRF. In addition, separating out the water continuum improves our fit of the local line water transmittance. Later, the water continuum is factored into the total transmittance as a separate term.

For each layer l, the convolved layer-to-space transmittances are ratioed with transmittances in the layer above, $l-1$, to form effective layer transmittances for fixed (F), water (W), and ozone (O) as follows:

$$\begin{aligned} F_l^{eff} &= \frac{F_l}{F_{l-1}} \\ O_l^{eff} &= \frac{FO_l}{FO_{l-1}} \div \frac{F_l}{F_{l-1}} \\ W_l^{eff} &= \frac{FOW_l}{FOW_{l-1}} \div \frac{FO_l}{FO_{l-1}} \end{aligned} \tag{7}$$

Forming these ratios in the above manner reduce the errors inherent in separating the gas transmittances after the convolution with the instrument spectral response function. The total effective layer transmittance can be recovered as follows,

$$FOW_l^{eff} = F_l^{eff} \times O_l^{eff} \times W_l^{eff} = \frac{FOW_l}{FOW_{l-1}} \tag{8}$$

The convolution of a product of terms is in general not the same as the product of the terms convolved individually. However, the above formulation guarantees the product of all the layer transmittances from layer l to N exactly returns FOW_l, if the layer transmittances are exact.

The zeroth layer transmittance (i.e. when $l-1=0$) is taken to be exactly 1.0. The negative logarithm of these layer effective transmittances is taken to get effective layer optical depths,

$$\begin{aligned} k_{fixed} &= -ln(F^{eff}) \\ k_{ozone} &= -ln(O^{eff}) \\ k_{water} &= -ln(W^{eff}) \end{aligned} \tag{9}$$

which become the dependent variables in the fast model regression.

Predictors The independent variables in the fast model regression, called the predictors, are a set of variables relating to the atmospheric profile. The optimal set of predictors used to parameterize the effective layer optical depth depends upon the gas, the instrument SRFs, the range of viewing angles, the spectral region, and even the layer thicknesses. In short, no one set of predictors is likely to work well in every case. Finding the set of predictors which give the best results is, in part, a matter of trial and error. However, there are some general trends.

For an instrument such as AIRS with thousands of channels, it is difficult to develop individual optimal predictors for each channel. The AIRS-RTA uses seven sets of predictors, each corresponding with a subset of channels. These sets of predictors were determined by extensive trial and error testing, as well as consideration of the relative importance of the variable gases in each channel. Supplemental sets of predictors are used for OPTRAN water, the water continuum, and variable CO_2.

The regression is prone to numerical instabilities if the values of the predictors vary too greatly. Consequently, we follow the usual practice of defining the predictors with respect to the values of a reference profile, either by taking a ratio or an offset. There is also a danger of numerical instability in the results of the regression, due to the interaction of some of the predictors. Sensitivity of the output to small perturbations in the predictors is avoided by systematic testing, but there are practical difficulties in detecting small problems since we are performing on the order of 1 million regressions.

As an example, the predictors for the fixed gases for one of the seven sets are shown:

$$1)a \;\; 2)a^2 \;\; 3)aT_r \;\; 4)aT_r^2 \;\; 5)T_r \;\; 6)T_r^2 \;\; 7)aT_z \;\; 8)aT_z/T_r \tag{10}$$

where a is the secant of the local path angle, T_r is the temperature ratio $T_{profile}/T_{reference}$, and T_z is the pressure weighted temperature ratio above the layer

$$T_z(l) = \sum_{i=2}^{l} P(i)(P(i) - P(i-1))T_r(i-1) \tag{11}$$

where $P(i)$ is the average layer pressure for layer l. The predictors for the variable gases can involve more complicated dependencies on the gas and the pressure weighted gas ratios above the layer, similar

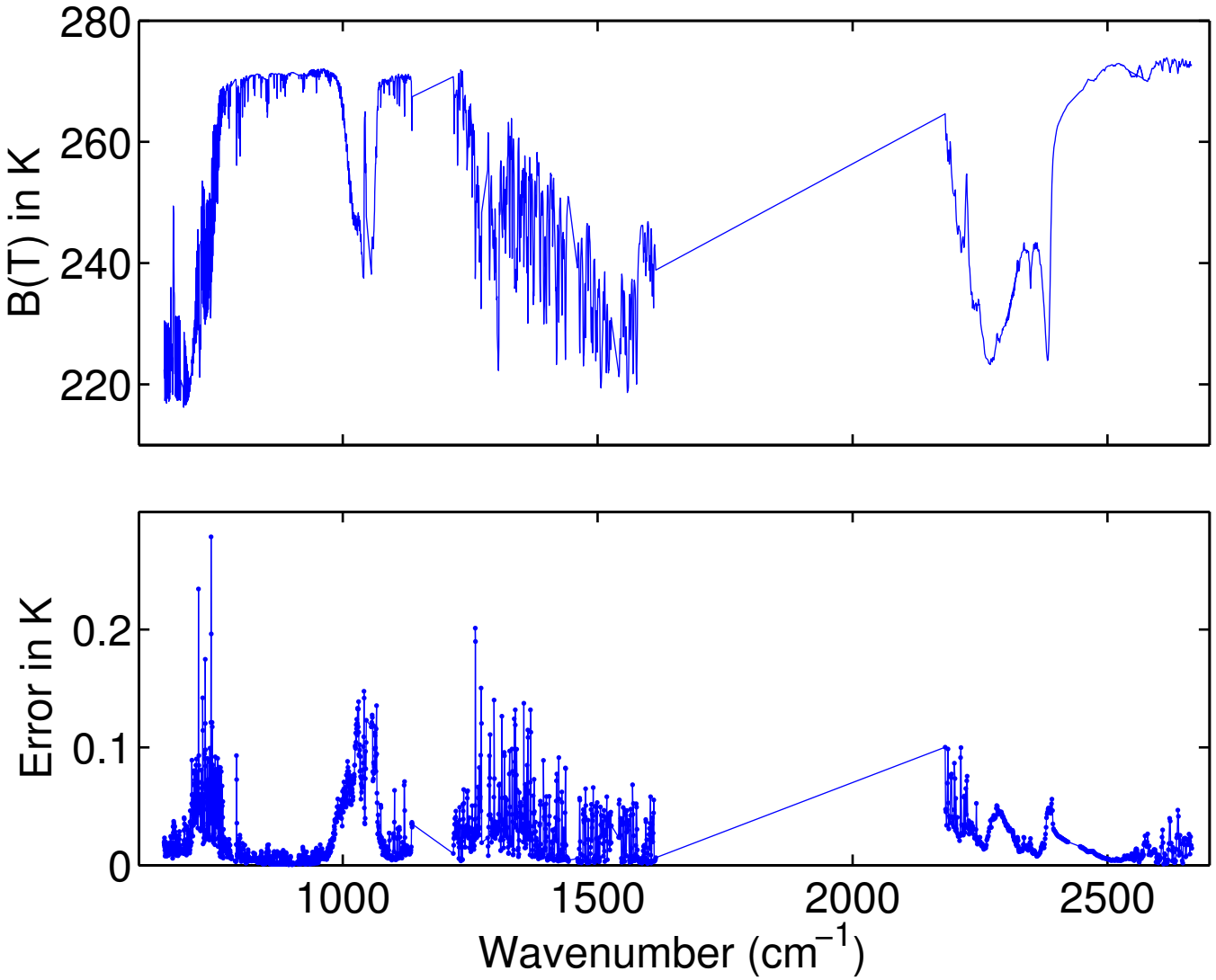

Figure 4: RMS Fitting errors of the AIRS-RTA Model.

to the temperature term defined above. Note that terms like T_z (or W_z, etc. for the variable gases) make the layer l transmittance dependent on the temperature (or gas amounts) in the layers above l.

Regressions for Fast Transmittance Parameters The accuracy of radiative transfer calculations made with the AIRS-RTA model was improved significantly by weighting the variables prior to performing the regression. Radiative transfer is insensitive to layers for which the change in layer-to-space transmittance across the layer is approximately zero. This occurs when either the layer effective transmittance is approximately unity, or the layer- to-space transmittance is approximately zero. Therefore, the data going into the regression is not all of equal importance to the final accuracy of radiative transfer calculations made with the model. We found it useful to weight the data in terms of both its effective layer optical depth as well as the total optical depth of all the layers above the layer under consideration.

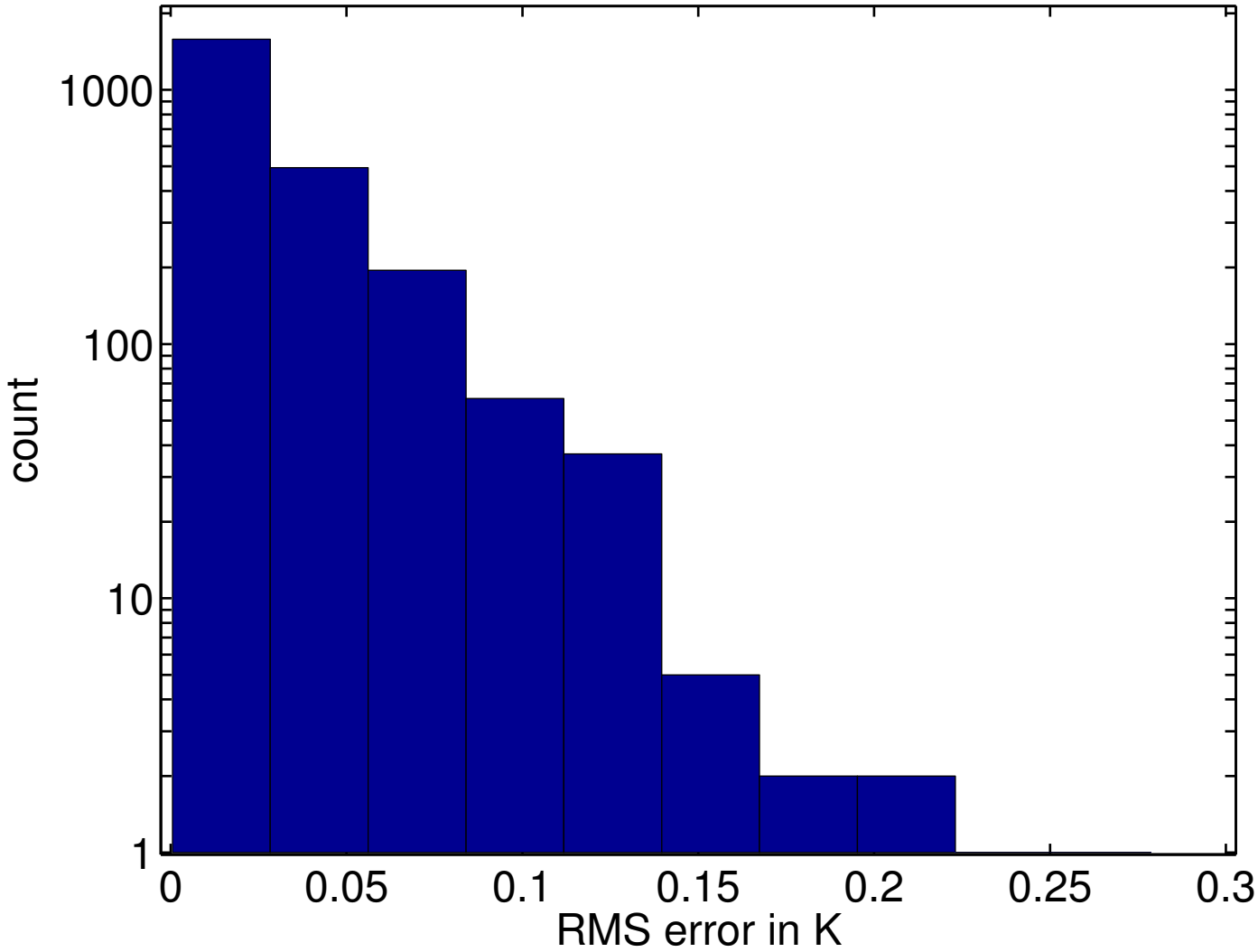

Figure 5: Histogram of the AIRS-RTA Model fitting errors for all channels.

The spectral dependence of the fitting errors are shown in Figure 4 and a histogram of these errors in Figure 5. The errors are calculated with respect to the regression profile set, comparing the RMS errors between the brightness temperatures of input data and the AIRS-RTA model calculated values. These graphs including errors from all six angles used for regression profiles. They do not include errors associated with the parameterization of the reflected thermal and reflected solar radiation.

During the development of the AIRS-RTA, the RMS errors were computed for a large independent set of profiles. The RMS errors for the independent profiles were generally similar to those for the regression profiles. The regression profiles represent a wide range of possible conditions, with a number of extreme cases. It is important to recognize, however, that the AIRS-RTA does have a statistical component that comes from the selection of the regression profiles.

Regression Profiles One other necessary pre-processing step is the selection of a set of profiles for calculation of the layer-to-space transmittances. The transmittances for these profiles become the regression data for the fast transmittance coefficients. These profiles should span the range of atmospheric variation, but, on the whole, should be weighted towards the more typical cases. The range of variation provides the regression with data points covering the range of possible atmospheric behavior, while the weighting of the mix of profiles towards more typical cases produces a transmittance model that works best on more statistically common profiles.

The process of calculating and convolving monochromatic layer-to-space transmittances is generally computationally intensive, thus imposing a practical limit on the number of profiles one can calculate for use in the regression. As discussed earlier, 48 regression profiles (at 6 viewing angles each) are sufficient to cover most of the profile behavior. This number is a compromise between the available time and computing resources and the need to cover a wide range of profile behavior in the regression. Choosing too few profiles leads to accuracy problems for profiles outside the range of behaviors considered. Choosing more profiles than necessary does not hurt the fast model, but does consume extra time and computer resources.

Each profile should cover the necessary pressure (altitude) range with data for temperature as well as absorber amount for each of the gases allowed to vary. The fixed gases include all whose spatial and temporal concentration variations have a negligible impact on the observed radiances. As previously mentioned, the variable gases are H_2O, O_3, CO, CH_4, and CO_2. All other gases are included in the "fixed gases". CO_2 is handled differently than the other variable gases, and only two CO_2 absorber amount profiles are used: a standard amount profile and a perturbed amount profile. The standard amount CO_2 profile is treated as a fixed gas. A very simple and accurate parameterization is used to model the difference in transmittance between the standard CO_2 profile transmittances and the perturbed CO_2 profile transmittances.

For those satellite viewing angles relevant to the AIRS instrument (0 to 49 degrees), the effects of viewing angle can be approximated fairly well by multiplying the nadir optical depth by the secant of the local path angle. This approximation neglects the minor refractive effect at large angles. Due to the curvature of the Earth, the local path angle is in general not the same as the satellite viewing angle, but is related to it by a fairly simple equation. Local atmospheric path angles of 0, 32, 45, 53, 60, and 63 degrees are used in the regression profiles to cover the 0- 49 degree satellite view angle range. An

additional six angles between 69-84 degrees are used for the shortwave channels where transmittances at large angles are need to model the reflected solar radiance.

4.2.3 Spectroscopy

The ultimate goal is to produce an AIRS-RTA that does not introduce significant errors in AIRS computed radiances. This requires a fast model that can compute accurate transmittances. Even if the fast model RMS fitting errors are zero, the accuracy of the transmittances are dependent upon the quality of the spectroscopic line parameters and lineshape models used to compute the monochromatic transmittances.

Due to the dominance of either CO2 or H2O absorption in the majority of AIRS channels, the most important spectroscopy errors are associated with errors in the line parameters and line shapes of these two gases. The line parameters most likely to introduce spectroscopy errors into the fast forward model for AIRS are the line strengths, line widths, and the temperature dependence of the line widths. However, errors in spectral lineshapes and continuum absorption probably are generally more troublesome than line parameter errors.

Currently, the HITRAN-2000 [Rothman et al., 2003] database is used for most atmospheric line parameters. As so many bands and molecules contribute to the observed radiances, the accuracy of the existing line parameters is difficult to judge in detail. Based upon our analysis of AIRS observations and calcuated radiances, we estimate the combined effects of line parameter and lineshape model errors in the computed optical depth of the stronger absorbing "fixed" gases (which in most spectral regions is dominated by CO_2) are typically at the 5% level, while for water the optical depth errors are at the 10% level.

Errors in the spectral lineshapes of CO2 and H2O are much more problematic than line parameter errors. Because of the large optical depths of CO2 and H2O in the atmosphere, their spectral line wings can be important, especially for remote sensing of temperature and humidity. For example, AIRS channels with the sharpest weighting functions are located in between lines or in the line wings where knowledge of the spectral line shape is most important. Moreover, accurate measurements of the line wing absorption are exceedingly difficult due to problems simulating atmospheric optical depths in a laboratory cell, especially for H2O. It is also tedious and expensive to make these large optical depth measurements at the low temperatures found in the upper troposphere.

Figure 6 shows the optical depth "tuning" used with the AIRS-RTA in version 4 processing. These multipliers are used to scale the indicated component of the optical depth inside the AIRS-RTA. These are empirically determined values, and some small portion of these adjustment may be due to error sources other than spectroscopy. Tracing these adjustments back to line parameter errors is no simple task and has not yet been attempted.

Figure 7 shows the effects of our optical depth tuning on AIRS radiances. The data set consists of the clearest night-time AIRS observations matched with sondes launched as part of the AIRS validation campaign. The sonde profiles were used with the AIRS-RTA to compute simulated radiances, which were then differenced with the observations. The sonde data did not extend to the stratosphere, so

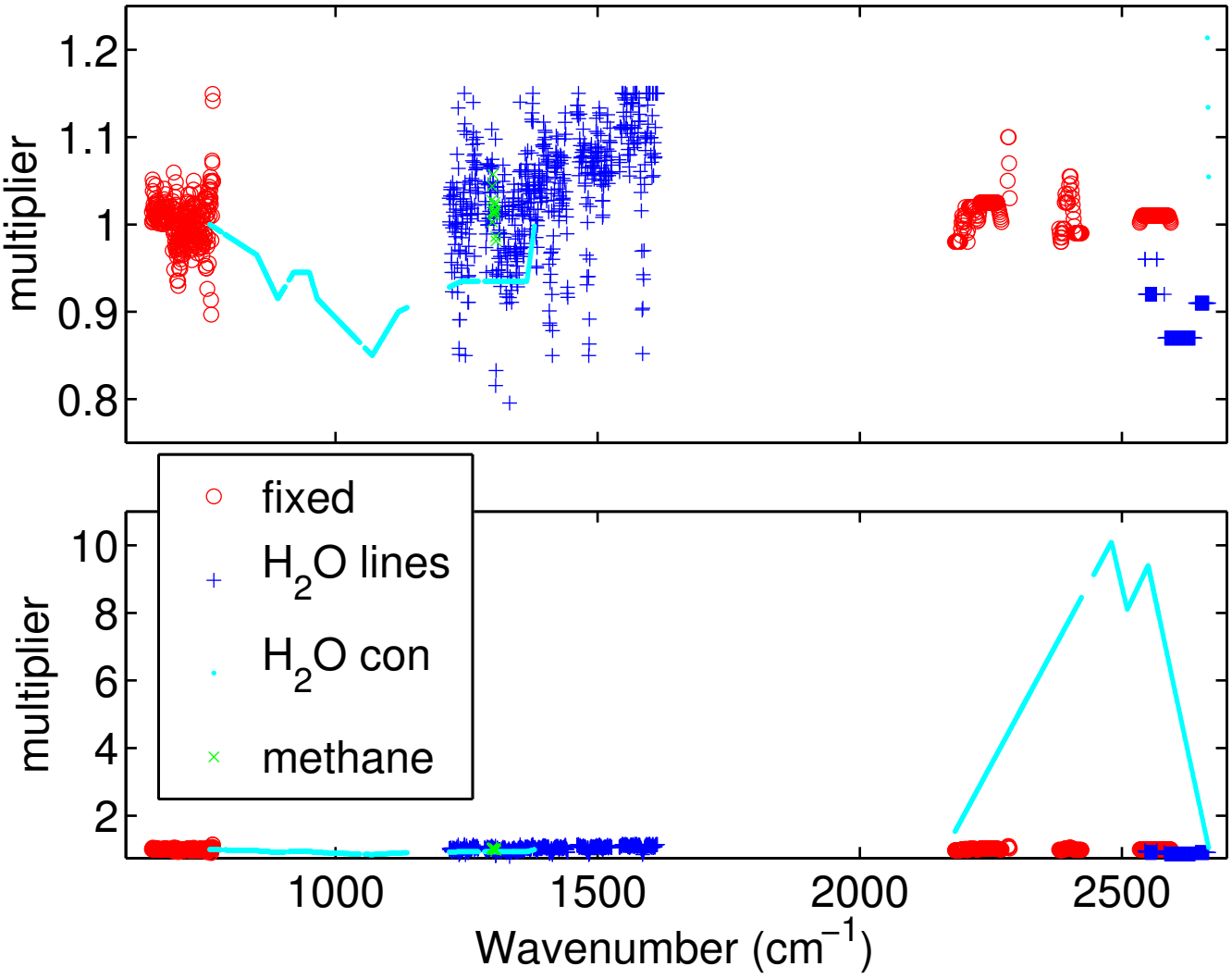

Figure 6: Optical depth tuning used in the V4 AIRS-RTA. The bottom panel shows the same data as the top panel, but with the vertical range expanded to illustrate the large adjustment to the water continuum in the shortwave channels.

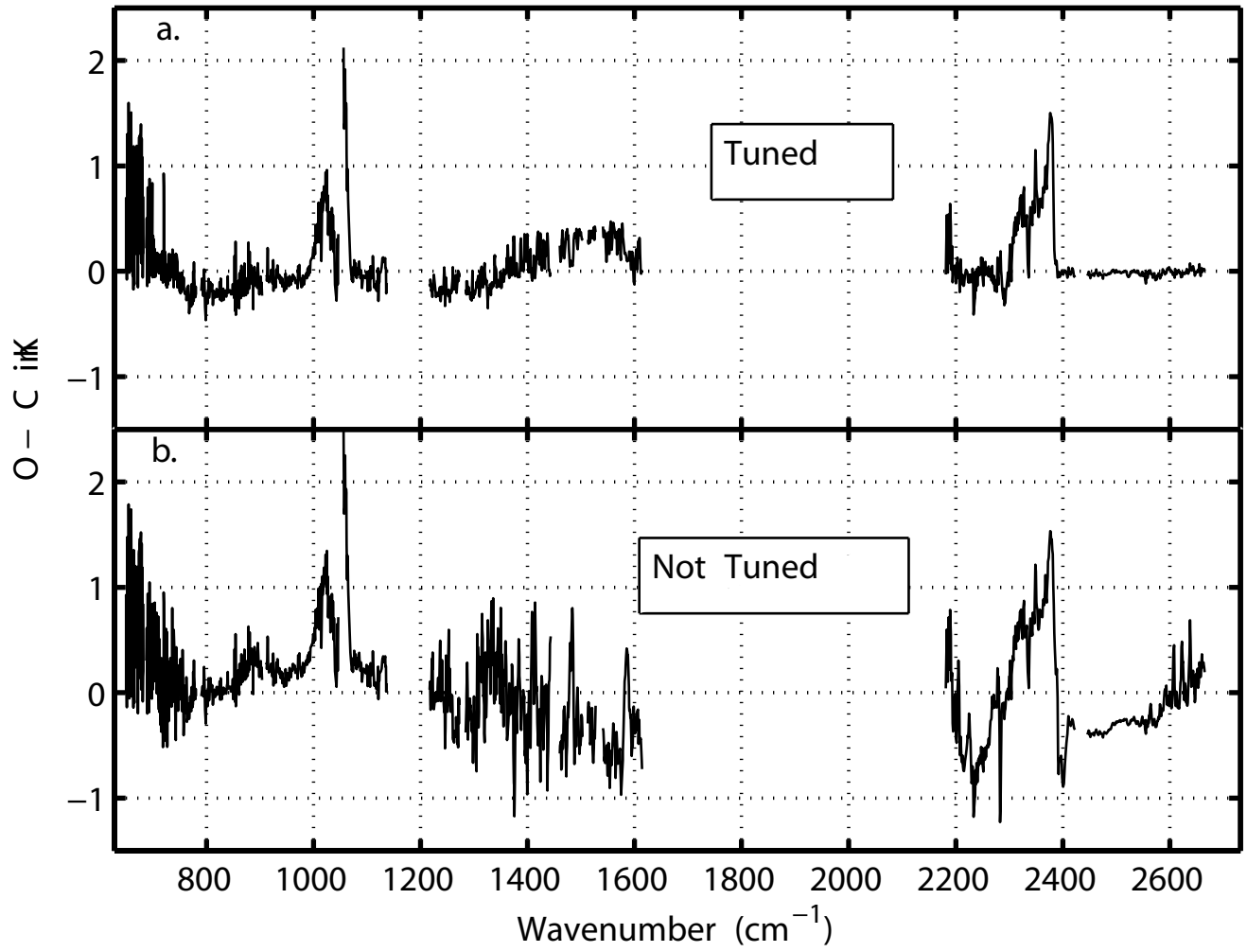

Figure 7: Comparison of observed - calculated brightness temperatures with and without optical depth tuning

ignore the bias in the 15 μm and 4.3 μm stratospheric channels. We solved for an effective surface skin temperature using the AIRS super-window channel at 2616 cm^{-1}, so the bias there has been forced to zero.

4.2.4 Monochromatic Transmittance Calculations

The monochromatic layer-to-space transmittances used to determine the parameters of the AIRS-RTA model are indirectly generated using our custom line-by-line code (UMBC-LBL). Building a custom LBL code allowed us to incorporate those features we deemed desireable, include our Q-, P-, and R-branch CO_2 line-mixing model which has a significant effect on the optical depths in the 15 μm and 4 μm regions.

Currently, 48 profiles are used in the regressions for the fast transmittance parameters. Because line-by-line (and especially Q/P/R branch line mixing) calculations are very slow, we developed a new pseudo line-by-line algorithm called the kCompressed Atmospheric Radiative Transfer Algorithm (kCARTA) to allow the (relatively) fast computation of almost monochromatic transmittances and radiances. The UMBC-LBL was used to compute a very large look-up table of monochromatic layer optical depths for a set of 11 reference atmospheric profiles. The kCARTA program interpolates the lookup table optical depths for temperature and scales for absorber amount to compute the optical depths for the desired profile. Any change in the physics of the line-by-line code or line parameter database requires a recalculation of the affected portion of the look-up table.

The kCARTA database consists of many individual look-up tables each covering a 25 cm^{-1} interval with 10,000 points (0.0025 cm^{-1} spacing) for 100 pressure layers (0.009492 to 1085 mb) and 11 temperatures. The 11 temperature profiles are the U.S. Standard profile, and 10 profiles offset from it in $\pm$ 10 K increments. On average, 7 gases must be included per 25 cm^{-1} region. The continua due to gases such as N_2 and O_2 are also included in these tables. Optical depths are computed using a 0.0005 cm^{-1} grid and then averaged to the database grid spacing of 0.0025 cm^{-1}. Consequently, the highest altitude optical depths are not truly monochromatic, but exhibit good integrated optical depths. The relatively large width of the AIRS Spectral Response Function (SRF) results in negligible errors due to this averaging.

This large look-up table has been compressed using a Singular Value Decomposition (SVD) method. The approximately 50 times compression achieved in kCARTA is lossy, but the accuracy of the transmittances remains very high. kCARTA bridges the gap between slow but accurate line-by-line codes, and fast but special purpose fast transmittance codes. kCARTA is used to calculate the 48 profile transmittances we use as regression data for the AIRS fast transmittance model. The computation time for these transmittances is not a significant fraction of the time involved in creation of a new fast model. However, the transmittance data files are very large, and the convolution of these monochromatic transmittances with the AIRS SRFs is a time consuming process.

4.2.5 Spectral Response Function Measurements and Modeling

Inaccuracies in the AIRS spectral response function directly impact the accuracy of the AIRS-RTA, and consequently the accuracy of the AIRS retrieved products. The AIRS SRFs are not Level 1 products, so it is appropriate to discuss the determination of the SRF functions in this document. Complete knowledge of the AIRS SRFs derived solely from ground calibration was not possible for two reasons; (1) small changes in the alignment of the AIRS spectrometer/focal plane since launch have shifted the centroids of the AIRS SRFs, and (2) the spectral location of fringes produced by the AIRS entrance aperture filters are dependent on the thermal environment of AIRS in orbit. Both of these effects to be relatively small, but our requirements on SRF knowledge are quite stringent.

Since becoming operational in late August 2002, the AIRS channel centroids have remained stable to within 1% of a channel Full Width at Half Maximum (FWHM). An extreme solar event in late October 2003 led mission control to shut off the AIRS coolers temporarily. When AIRS was switched back on in early November 2003, it required a few weeks to cool down, and then be re-calibrated back to approximately the same configuration as before the shutdown. While it was possible to adjust the channels back to their pre-shutdown centroids, this required a small change to the operating temperature, which resulted in a small relative shift of the fringes. The effects of this shift are small enough to ignore for retrieval purposes, but may need to be accounted for when looking at radiance biases for climate purposes.

Figure 8 shows the estimated change to a the AIRS observed brightness temperatures due to the change in fringe position in November 2003. The effects are negligible in most channels, but not everywhere. The largest change is in 2200 cm^{-1} region which affects the CO sonding channels. The inset plot shows a blowup of this region, and the good agreement between the model and observed change is evidence the fringe and SRF models are fairly accurate.

While we can not measure the SRFs in orbit, we can measure the channel centroids to fairly high accuracy. Careful analysis of AIRS data indicates the channel centroids drift back and forth by $\sim$ 0.5% of a FWHM (peak-to-peak) over each orbit. The exact reason for this drift is uncertain, but it is probably related to solar heating effects. There is also a long term drift, with the channels having drifted $\sim$ 0.3% of a FWHM in the first two years since launch. This slow drift appears to be slowing and it may not be necessary to take action to maintain the current channel centroids. If it is eventually deemed necessary, it should be possible to again "dial in" the original channel centroids by adjusting the temperature of the focal plane, but this would again cause another relative shift in the fringe positions.

Figure 9 shows the drift in the AIRS channel centroids as a function of time as well as latitude during the ascending (day-time) portion of Aqua's orbit. The back-and-forth shift of the centroids with each orbit shows up in this plot as the latitude dependence of the shift. The data used for this plot does not extend to high latitudes, so the full range of the shift with latitude is not shown.

The Version 4 AIRS-RTA and Level 1B data does not account for this small orbital and long-term centroid drift. The effects of a 0.5% error in the channel centroids is shown in figure 10. It is possible to apply an approximate correction for a small centroid error by interpolating the forward model radiances, but that requires knowledge of the centroid position.

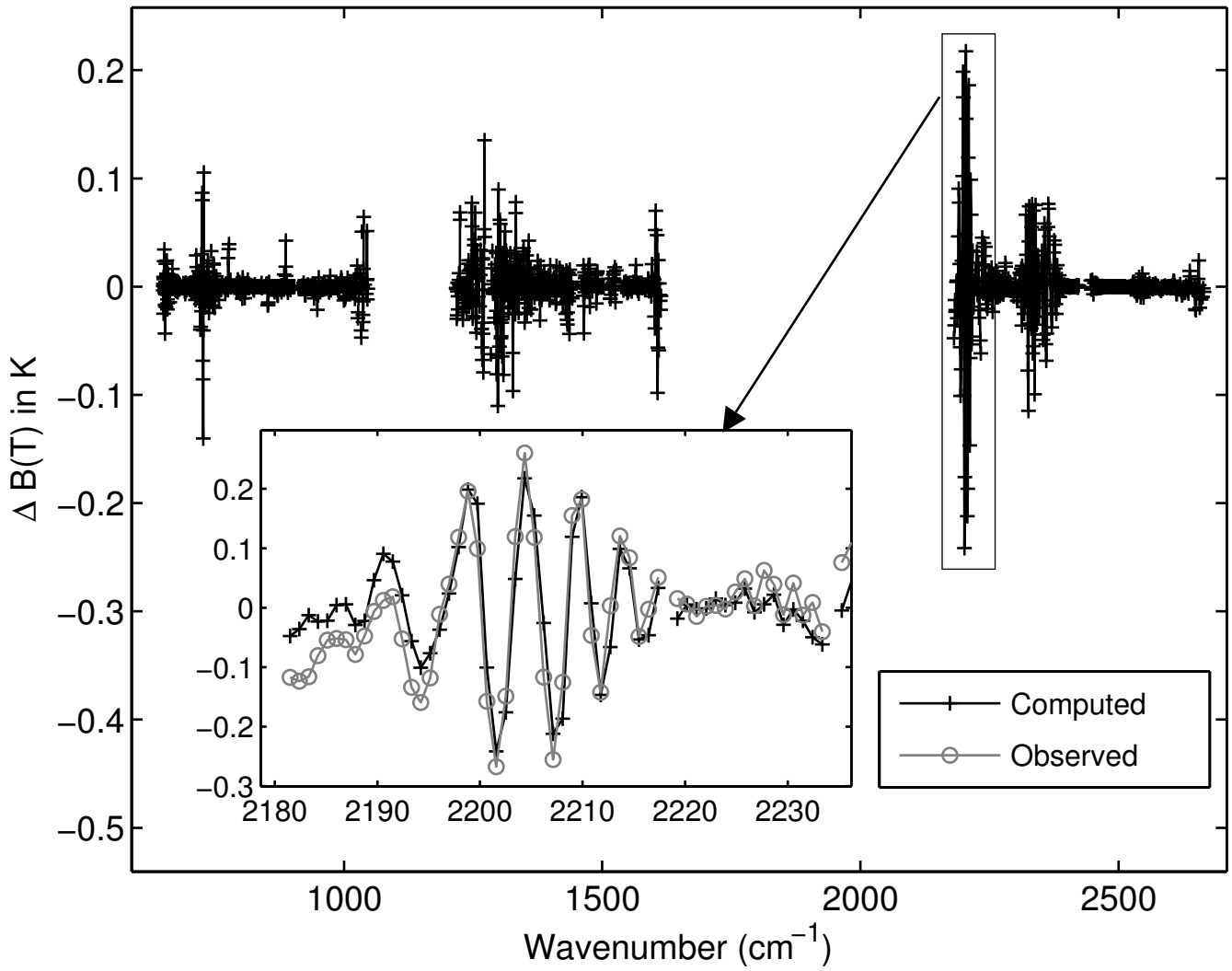

Figure 8: Estimated change to AIRS observed brightness temperatures due to the offset in fringe position in November 2003

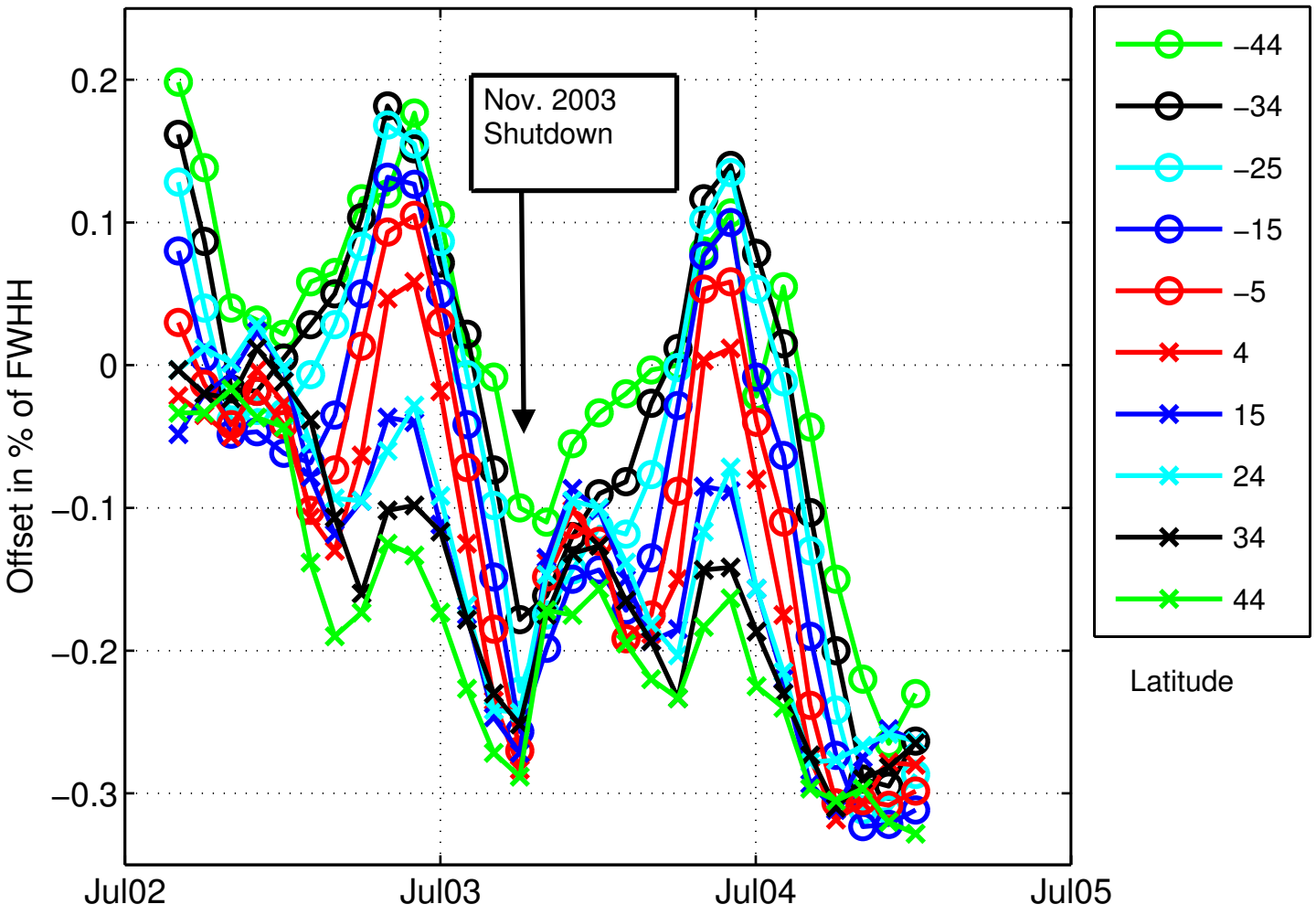

Figure 9: Centroid drift versus time and latitude; ascending (day) orbit

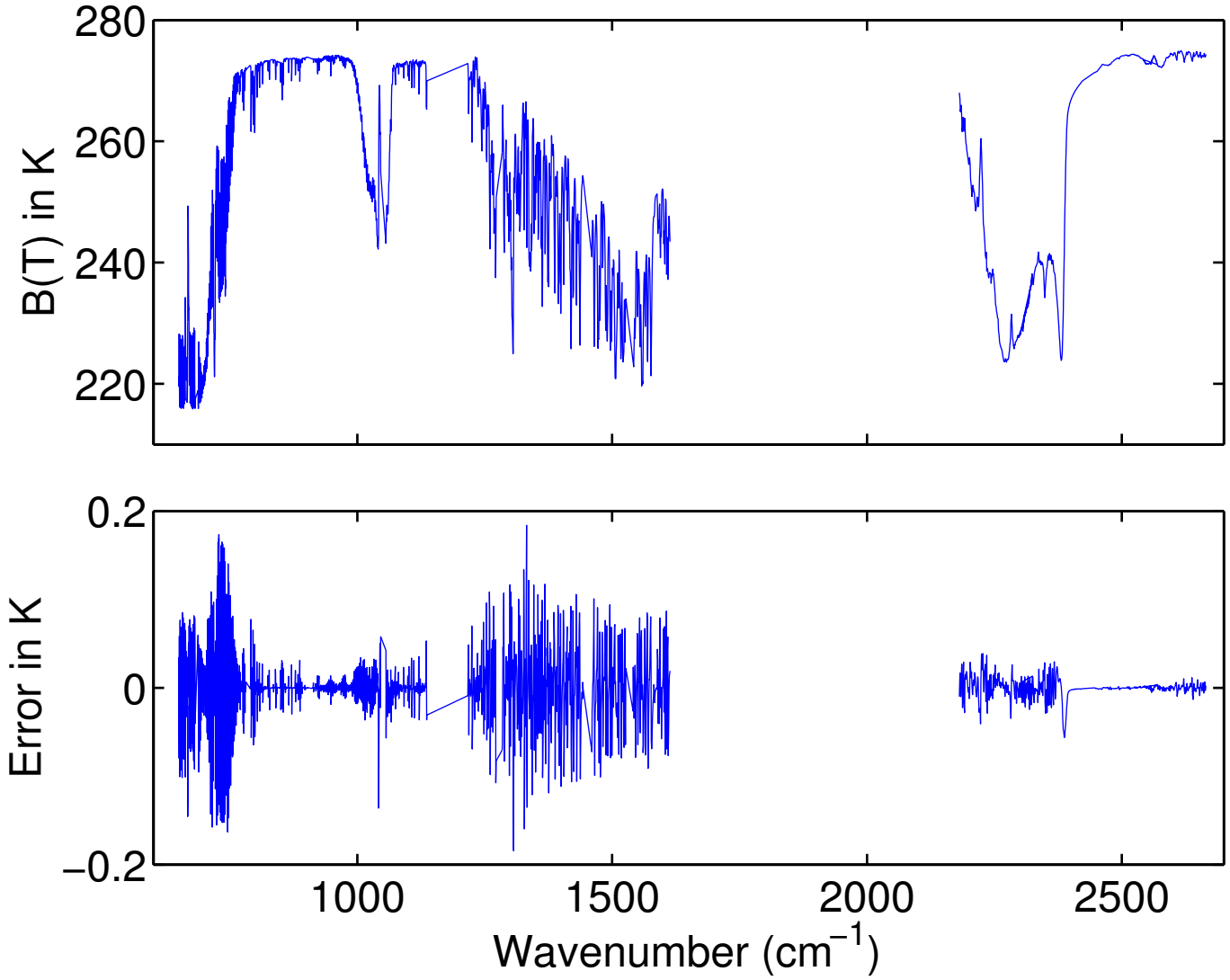

Figure 10: Brightness temperature error for a 0.5% error in channel centroids

4.2.6 AIRS-RTA Error Analysis

The following table contains rough estimates of the errors in the AIRS-RTA in units of brightness temperature. They are separated into radiative transfer/spectroscopy errors and SRF knowledge errors. In many cases these errors will be correlated, sometimes of opposite sign. Consequently it is very difficult to properly combine the errors in Table 4.2.1 into a single AIRS-RTA error budget. In addition, most of these errors are highly channel dependent. They have been estimated conservatively and represent upper bounds.

Radiative Errors	Error (K)	Comment
Fast model fit	0.05 - 0.3	Can be larger for individual profiles
Spectroscopy	0.2 - 0.6	Errors are more likely for water
Reflected thermal	0.0 - 0.2	Proportional to reflectivity
Solar	0.0 - 0.1	Can be much larger if ρ is off
Layering	0.05	Most channel have lower errors
Polychromatic approximation	0.05	Most channel have lower errors
Aerosols	0.0 - 1	Dust can make it thru cloud clearing
SRF Errors		
Centroids	0.0 - 0.1	Possible to corrected for
Widths	0.0 - 0.2	Negligible for most channels
Fringes	0.0 - 0.2	Negligible for most channels
Wings	0.0 - 0.2	negligible for most channels